

HEPHY-PUB 700/98  
STPHY 30/98

**MULTIPLICITY DEPENDENCE OF LIKE-SIGN AND  
OPPOSITE-SIGN CORRELATIONS IN  $\bar{p}p$  REACTIONS**

B. BUSCHBECK\*, H.C. EGGERS† and P. LIPA\*

\* *Institut für Hochenergiephysik, Nikolsdorfergasse 18, A-1050 Vienna, Austria*

† *Department of Physics, University of Stellenbosch, 7600 Stellenbosch, South Africa*

**Abstract**

Discussions about Bose-Einstein correlations between decay products of coproduced W-bosons again raise the question about the behaviour of correlations if several strings are produced. This is studied by the multiplicity dependence of like-sign and opposite-sign correlations in  $\bar{p}p$  reactions at  $\sqrt{s} = 630$  GeV.

---

To be published in Proceedings of the 8<sup>th</sup> Internat. Workshop on Multi-particle Production “Correlations and Fluctuations” in Mátraháza, Hungary, Eds.: T. Csörgö, S. Hegyi, R.C. Hwa and G. Jancsó, World Scientific.

## 1 Introduction

Recently, there has been much discussion regarding the possibility that Bose-Einstein correlations and other interconnection effects<sup>1</sup> between decay products of different strings could affect the measurement of the  $W$  mass. Since measurements are hampered by low statistics and experimental difficulties, the question arises whether and where effects of the superposition of several strings can be tested independently. Within the Dual Parton Model, the number of strings may be expected to be proportional to multiplicity and thus influence the multiplicity dependence of various effects, in particular Bose-Einstein correlations. While the decrease in observed  $\lambda$  as function of multiplicity can be explained naturally in terms of products of different strings,<sup>2,3</sup> other features such as the radius cannot.<sup>4</sup>

Improvements in experimental analysis techniques,<sup>5</sup> larger data samples and the above theoretical background make it desirable to repeat and extend Bose-Einstein analyses with an advanced strategy. In this contribution, we investigate like-sign and opposite-sign correlations at different total multiplicities with the same model-independent strategy and good statistics. The bias introduced by selecting events of a given overall multiplicity is eliminated with the use of “internal cumulants”.<sup>5</sup>

## 2 Data sample and normalized density correlation functions

The data sample consists of 600.000 non-single-diffractive  $\bar{p}p$  reactions at  $\sqrt{s} = 630$  GeV measured by the UA1 central detector.<sup>6</sup> As before, only vertex-associated charged tracks with transverse momentum  $p_T \geq 0.15$  GeV/c,  $|\eta| \leq 3$ , good measurement quality and fitted length  $\geq 30$ cm have been used. To avoid acceptance problems, we restricted the azimuthal angle to  $45^\circ \leq |\phi| \leq 135^\circ$  (“good azimuth”).

Fig. 1 shows the normalized density correlation functions for pairs of like-sign charge and for opposite-sign charge separately. Restricting the total uncorrected charged multiplicity  $N$  in  $|\eta| \leq 3$  to the windows  $1 \leq N \leq 6$  (Fig. 1a) and  $28 \leq N \leq 35$  (Fig. 1b), one obtains for the corrected particle density in the central rapidity region  $dn/d\eta = 0.83 \pm 0.08$  and  $dn/d\eta = 5.3 \pm 0.17$  respectively<sup>a</sup>. All quantities measured are defined in the notation of correlation

---

<sup>a</sup>Events are selected according to multiplicity in *all azimuthal* regions, while the subsequent analysis is performed for particles in the *good azimuth* only. This is done because the total rather than the good-azimuth multiplicity is physically relevant. Total multiplicity density ( $dn/d\eta$ ) is estimated as twice the density measured in the good-azimuth region.

integrals<sup>7</sup>,

$$r_2(Q) = \frac{\rho_2(Q)}{\rho_1 \otimes \rho_1(Q)} = \frac{\int_{\Omega} d^3 \mathbf{p}_1 d^3 \mathbf{p}_2 \rho_2(\mathbf{p}_1, \mathbf{p}_2) \delta [Q - q(\mathbf{p}_1, \mathbf{p}_2)]}{\int_{\Omega} d^3 \mathbf{p}_1 d^3 \mathbf{p}_2 \rho_1(\mathbf{p}_1) \rho_1(\mathbf{p}_2) \delta [Q - q(\mathbf{p}_1, \mathbf{p}_2)]}$$

with  $\mathbf{p}$  the three-momenta and  $q \equiv \sqrt{-(p_1 - p_2)^2}$ , with  $p$  being the corresponding four-momenta. The integration region  $\Omega$  is identical with our experimental cuts as specified above. All particles have been assumed to be pions.

In  $\bar{p}p$  reactions and in full phase space the number of positive and negative particles are equal; furthermore in the central rapidity region the corresponding  $\rho$ -functions are also equal. Given the charged multiplicity  $\rho_1(\mathbf{p}) = \rho_1^+(\mathbf{p}) + \rho_1^-(\mathbf{p})$ , we hence assume that  $\rho_1^+(\mathbf{p}) = \rho_1^-(\mathbf{p}) \simeq \frac{1}{2}\rho_1(\mathbf{p})$  and therefore also  $\rho_1^+ \otimes \rho_1^+(Q) \simeq \frac{1}{4}\rho_1 \otimes \rho_1(Q)$  etc. The like-sign and opposite-sign normalised correlation densities hence become, respectively,

$$r_2^{\ell s}(Q) = \frac{\rho_2^{\pm\pm}(Q)}{\rho_1^{\pm} \otimes \rho_1^{\pm}(Q)} = \frac{\rho_2^{++}(Q) + \rho_2^{--}(Q)}{\rho_1^+ \otimes \rho_1^+(Q) + \rho_1^- \otimes \rho_1^-(Q)} \simeq \frac{\rho_2^{++}(Q) + \rho_2^{--}(Q)}{\frac{1}{2}\rho_1 \otimes \rho_1(Q)},$$

$$r_2^{os}(Q) = \frac{\rho_2^{\pm\mp}(Q)}{\rho_1^{\pm} \otimes \rho_1^{\mp}(Q)} = \frac{\rho_2^{+-}(Q) + \rho_2^{-+}(Q)}{\rho_1^+ \otimes \rho_1^-(Q) + \rho_1^- \otimes \rho_1^+(Q)} \simeq \frac{\rho_2^{+-}(Q) + \rho_2^{-+}(Q)}{\frac{1}{2}\rho_1 \otimes \rho_1(Q)}.$$

In Fig. 1, both the like-sign and opposite-sign correlation densities show a strong dependence on multiplicity. To perform, however, a quantitative analysis, one has to get rid of the combinatorial background by calculating the cumulants and secondly to correct for the bias introduced by fixing multiplicity<sup>b</sup>.

### 3 Cumulants for limited multiplicity ranges

A quantitative study of the bias introduced by fixing multiplicity has been performed by Lipa et al.<sup>5</sup> At fixed total multiplicity  $N$ , the standard factorial cumulants

$$\kappa_2(\mathbf{p}_1, \mathbf{p}_2 | N) = \rho_2(\mathbf{p}_1, \mathbf{p}_2 | N) - \rho_1(\mathbf{p}_1 | N) \rho_1(\mathbf{p}_2 | N) \quad (1)$$

are nevertheless nonzero, even when particles are completely uncorrelated. These purely “external” correlations appear because the cumulant for any multinomial distribution is nonzero; for example, in second order,

$$\kappa_2^{\text{mult}}(\mathbf{p}_1, \mathbf{p}_2 | N) = -\frac{1}{N} \rho_1(\mathbf{p}_1 | N) \rho_1(\mathbf{p}_2 | N). \quad (2)$$

<sup>b</sup> The usual Bose-Einstein analysis assumes that  $r_2^{\ell s}$  tends to a constant for large  $Q$ , ie.  $r_{2 \text{ BE}}^{\ell s}(Q \geq 1) = \text{constant}$ . It should be clear from Figure 1 that no such constancy exists for limited multiplicity windows.

As shown in Ref. <sup>5</sup>, the “internal cumulants”

$$\kappa_2^I(\mathbf{p}_1, \mathbf{p}_2 | N) \equiv \kappa_2(\mathbf{p}_1, \mathbf{p}_2 | N) - \kappa_2^{\text{mult}}(\mathbf{p}_1, \mathbf{p}_2 | N) \quad (3)$$

correct this bias exactly: they are zero whenever the  $N$  particles behave multinomially. Integrating (1)–(3) to obtain the correlation integral and normalizing, we arrive at the normalized internal cumulants for given fixed  $N$ ,

$$K_2^I(Q | N) = \frac{\kappa_2^I(Q | N)}{\rho_1 \otimes \rho_1(Q | N)} = r_2(Q | N) - \left(1 - \frac{1}{N}\right). \quad (4)$$

The prescription for calculating the  $K_2^I(Q | N)$  is therefore to measure at fixed  $N$  (in  $\Omega$ ) first  $r_2(Q | N) = \rho_2(Q | N) / \rho_1 \otimes \rho_1(Q | N)$  and then to subtract

$$1 - \frac{1}{N} = \frac{N(N-1)}{N^2} = \frac{\int_{\Omega} \rho_2(Q | N) dQ}{\int_{\Omega} \rho_1 \otimes \rho_1(Q | N) dQ}.$$

To obtain adequate statistics, we have to measure averages over limited multiplicity ranges rather than at fixed  $N$ . The internal second-order cumulant averaged over the multiplicity range  $[A, B]$  is given in <sup>5</sup> by

$$\overline{\kappa_2^I}(\mathbf{p}_1, \mathbf{p}_2) = \frac{\sum_{N=A}^B P_N \kappa_2^I(\mathbf{p}_1, \mathbf{p}_2 | N)}{\sum_{N=A}^B P_N}, \quad (5)$$

where  $P_N$  is the experimental multiplicity distribution in  $[A, B]$  and the bar over any quantity  $S$  denotes  $\overline{S} \equiv \sum_{N=A}^B P_N S(N) / \sum_{N=A}^B P_N$ . Assuming that the shape of  $\rho_1(\mathbf{p} | N)$  does not vary in  $[A, B]$

$$\rho_1(\mathbf{p} | N) \simeq (N/\overline{N}) \overline{\rho}_1(\mathbf{p}_1),$$

and adopting again the correlation integral prescription, we can write

$$\overline{K_2^I}(Q) = \frac{\overline{\kappa_2^I}(Q)}{\overline{\rho}_1 \otimes \overline{\rho}_1(Q)} = \frac{\overline{\rho}_2(Q)}{\overline{\rho}_1 \otimes \overline{\rho}_1(Q)} - \frac{\int_{\Omega} \overline{\rho}_2(Q) dQ}{\int_{\Omega} \overline{\rho}_1 \otimes \overline{\rho}_1(Q) dQ}. \quad (6)$$

For like-sign measurements, this becomes

$$\overline{K_2^{I\ell s}} = \frac{\overline{\rho_2^{\ell s}}(Q)}{\frac{1}{2} \overline{\rho}_1 \otimes \overline{\rho}_1(Q)} - \frac{\int_{\Omega} \overline{\rho_2^{\ell s}}(Q) dQ}{\frac{1}{2} \int_{\Omega} \overline{\rho}_1 \otimes \overline{\rho}_1(Q) dQ} \quad (7)$$

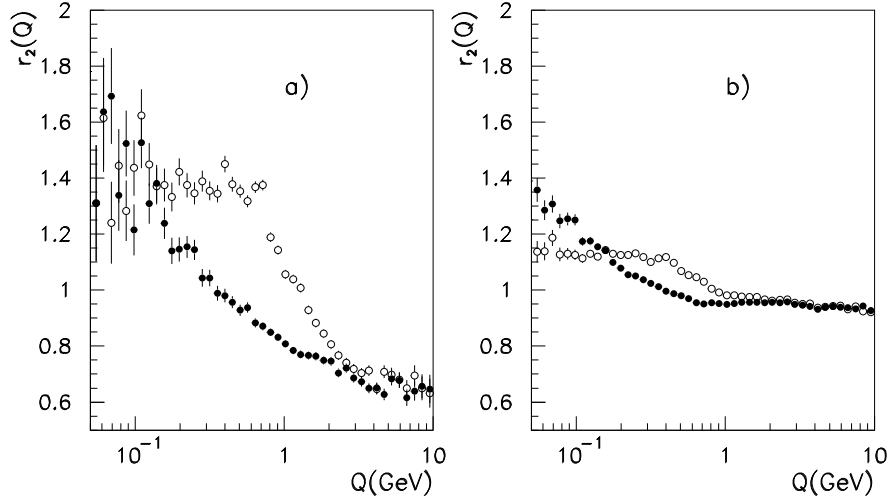


Figure 1:  $r_2^{\ell s}$  versus  $Q$  for like-sign pairs (full circles) and  $r_2^{os}$  versus  $Q$  for opposite-sign pairs (open circles) at a)  $dn/d\eta = 0.83$  and b)  $dn/d\eta = 5.3$ .

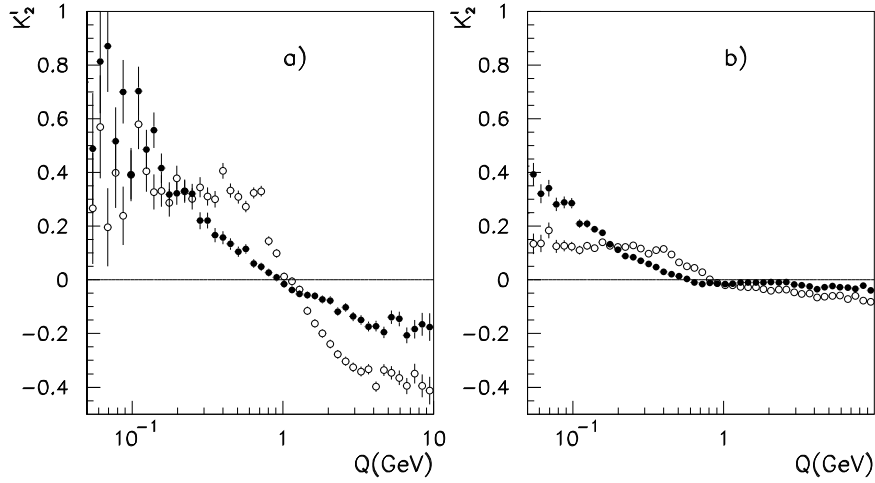


Figure 2: Internal cumulants eqns. (7) for  $\ell s$  pairs (full circles) and  $os$  pairs (open circles) for two different multiplicity densities, a)  $dn/d\eta = 0.83$  and b)  $dn/d\eta = 5.3$ .

and similarly for  $\overline{K_2}^{Ios}$ . Since all quantities shown here and below are to be understood as mean values in multiplicity ranges like in (5) – (7), we henceforth (and in Fig. 1) omit the bar on the symbols.

Fig. 2 shows both like- and opposite-sign internal cumulants for two selections of  $dn/d\eta$ . Three features are immediately apparent:

- I. The cumulants differ from the moments of Fig. 1 by a shift constant in  $Q$ , but the amount of the shift changes for different cumulants. The importance of changing from  $r_2$  to  $K_2^I$  lies in the fact that the latter demarcate clearly the “line of no correlation”.
- II. Internal cumulants integrate to zero over the entire phase space; hence the positive part of  $K_2^I$  at small  $Q$  is compensated by a negative part at larger  $Q$ . Physically, this means that particles like to cluster, so that there is a surfeit of pairs at small  $Q$  and a dearth of pairs at large  $Q$  compared to the uncorrelated case.
- III. The dependencies of the like- and opposite-sign cumulants on multiplicity are rather similar in that both decrease markedly with  $dn/d\eta$ . This is discussed below.

#### 4 Multiplicity dependence of normalized cumulants

The similar decrease of  $K_2^{I\ell s}$  and  $K_2^{Ios}$  with  $dn/d\eta$  suggests that both could have the same functional dependence on multiplicity density. Under this hypothesis,

$$\begin{aligned} K_2^{I\ell s}(Q, dn/d\eta) &= Y^{\ell s}(Q)C(dn/d\eta, Q), \\ K_2^{Ios}(Q, dn/d\eta) &= Y^{os}(Q)C(dn/d\eta, Q), \end{aligned} \quad (8)$$

the quotient of the cumulants should be independent of multiplicity

$$\frac{K_2^{I\ell s}(Q, dn/d\eta)}{K_2^{Ios}(Q, dn/d\eta)} = \frac{Y^{\ell s}(Q)}{Y^{os}(Q)} = \left( \text{constant in } \frac{dn}{d\eta} \right). \quad (9)$$

Figure 3a shows that (9) holds at least approximately within error bars. (In the region where both cumulants are near zero, no meaningful quotients can be formed.)

Having shown that like- and unlike-sign internal cumulants behave approximately in the same way as functions of  $dn/d\eta$ , we now ask how this dependence is structured. A first hypothesis, is that  $K_2^I$  depends inversely on  $N$ ; in the notation of Eq. (8),

$$K_2^{I^a}(Q|N) = Y^a(Q)C(N, Q) = Y^a(Q)N^{-1} \quad a = \ell s, os. \quad (10)$$

This can be motivated theoretically by

- a) **Resonances:** If the unnormalized cumulants  $\kappa_2^{I^{os}}$  and  $\kappa_2^{I^{\ell s}}$  were wholly the result of resonance decays and if the number of resonances were proportional to the multiplicity  $N$ , then  $\kappa_2^I \propto N$ . Assuming  $\rho_1(\mathbf{p}|N) \propto N\rho_1(\mathbf{p})$  gives  $\rho_1 \otimes \rho_1 \propto N^2$ , and hence after normalization, the resonance-inspired guess

$$K_2^I = \frac{\kappa_2^{I^{\text{res}}}}{\rho_1 \otimes \rho_1} \propto \frac{1}{N}.$$

- b) **Independent superposition** in momentum space of  $n$  equal strings would also lead to  $K_2^I = n \cdot \kappa_2^{I^{\text{string}}} / (\rho_1 \otimes \rho_1) \propto (1/n) \propto (1/N)$ . Deviations can occur if the strings are unequal.

Eq. (10) implies that  $K_2^{I^a}(Q|N_1)/K_2^{I^a}(Q|N_2) = (N_2/N_1) = (\text{constant in } Q)$  for two multiplicities  $N_1$  and  $N_2$ . In Fig. 3b, we show the quotient of cumulants for two multiplicities. Surprisingly, we find not one but two constants, one for small  $Q \lesssim 0.4$  GeV, one for large  $Q \gtrsim 2$  GeV, where only the latter corresponds to the value  $(N_2/N_1)$  expected from (10), shown as the dotted line. At small  $Q$ , one must clearly look for other functional forms for  $C(N, Q)$ . Some phenomenological guesses are as follows.<sup>8</sup>

- c) In the **source picture of Bose-Einstein** correlations, the independent superposition of sources in configuration space leads to  $K_2^{I, BE} \simeq \text{constant}$  in  $N$ . We would expect  $\lambda$  to be independent of multiplicity, but the radius  $R$  to increase with  $N$ . Hence there should be a change of shape of  $K_2^{I^{\ell s}}(Q)$  but no overall  $N$ -dependence.
- d) A mixture of processes, a) with c) could result in a dependence

$$K_2^{I^{\ell s}}(Q|N) \approx a(Q) + \frac{b(Q)}{N} \quad (11)$$

However, no comparable source picture is available for the unlike-sign case. Also, the quotient  $K_2^{I^{\ell s}}/K_2^{I^{os}}$  would not be constant in  $N$ , in contradiction to the results of Fig. 3a.

- e) Another guess would yield a  $N^{-1}$  dependence for large  $Q$ , while the small- $Q$  region scales with  $N^{-\alpha}$ , with a different “constant”  $Y_2$ ,

$$K_2^{I^a} = \frac{Y_1^a(Q)}{N} \Theta(Q - 2) + \frac{Y_2^a(Q)}{N^\alpha} \Theta(0.4 - Q) + \dots \quad a = \ell s, os, \quad (12)$$

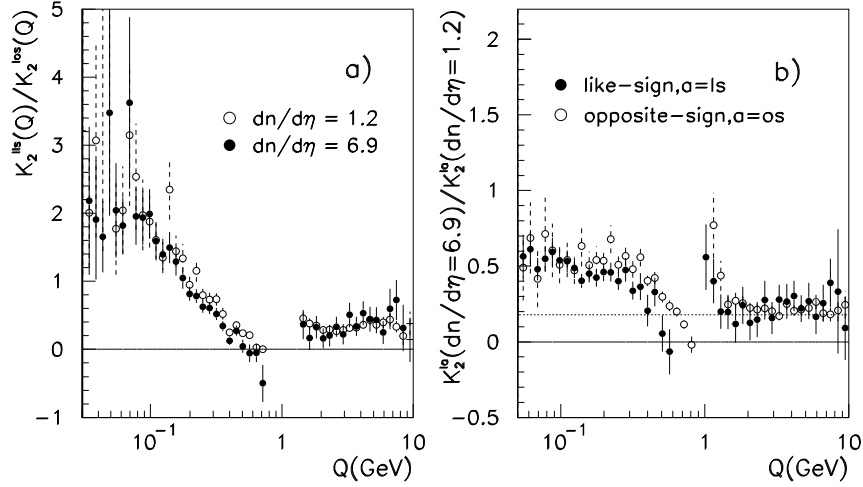


Figure 3: a) The ratio Eq. (9) is shown for two selections of  $dn/d\eta$ . b) The ratio of two  $K_2^{Ia}(Q)$  at different  $dn/d\eta$  as indicated on ordinate. The region around  $Q = 1$  has been omitted because the denominators are around zero.

In order to test the above ideas, we plot the cumulants against  $(dn/d\eta)^{-1}$  as follows. To avoid local statistical fluctuations, the normalized cumulants  $K_2^{I\ell s}(Q)$  and  $K_2^{Ios}(Q)$  are fitted with suitable functions in restricted  $Q$ -ranges (not shown). The  $K_2^{I\ell s}(Q)$  have also been fitted to an exponential parametrization for  $Q < 1$  GeV/c

$$K_2^{I\ell s}(Q) = a + \lambda e^{-RQ}. \quad (13)$$

The multiplicity dependence of the fitted  $K_2^{I\ell s}$  and  $K_2^{Ios}$  (circles), as well as the corresponding  $\lambda$  values (crosses) are plotted in Fig. 4. Fig. 4b shows that, as in Fig. 3b, the  $(1/N)$ -dependence is satisfied only for large  $Q$ , but not for small  $Q$ . The  $a+b/N$  dependence in Fig. 4a (solid line) provides a possible, but hardly unique, explanation. The dashed line corresponding to  $N^{-\alpha}$  behaviour (12) seems somewhat better. However, while this form is compatible with all results shown so far, we have no phenomenological justification for it. Eq. (12) also omits the region around  $Q \simeq 1$  GeV (e.g. the region of  $\rho^0$  production) where the phase space contributes maximally, but the  $K_2^{Ios}$  decrease rapidly with increasing  $Q$  and the  $K_2^{I\ell s}$  are already small (Fig. 2). It is difficult to investigate this important region directly. A  $1/N$  dependence (via resonances, for example) in the dominant region around 1 GeV/c could presumably cause the large- $Q$  region to follow suit via missing pairs.



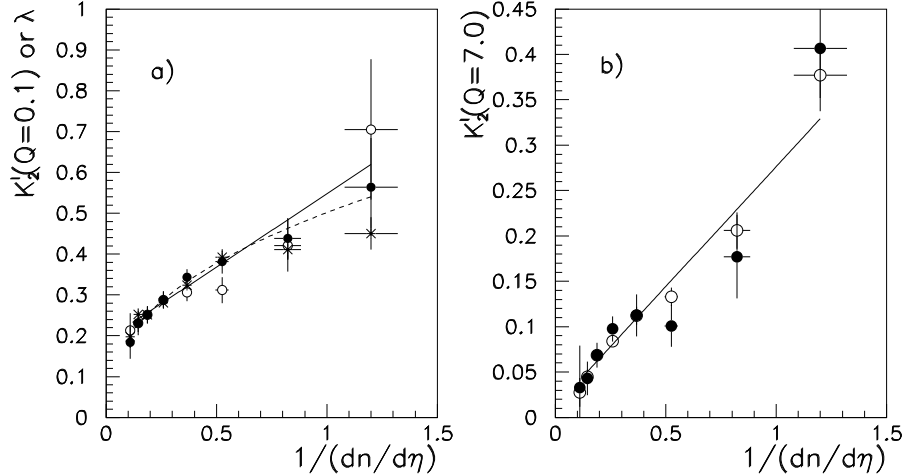


Figure 4: a) Multiplicity dependence of  $K_2^{I\ell s}(Q = 0.1)$  (full circles) and of  $K_2^{Ios}(Q = 0.1)$  (open circles) and  $\lambda$  values of exponential fit, Eq. (13) (crosses), b) as in a) but for the large  $Q$  region. For better comparison of the respective dependencies on  $dn/d\eta$ , the absolute values have been scaled by constant factors. The straight lines are linear fits, the dashed line corresponds to eqn.(12).

## 5 Summary

The multiplicity dependence of like-sign and opposite-sign two-body correlation functions are studied with the same model-independent strategy. The bias introduced by selecting events of a given overall multiplicity is eliminated in measuring “internal cumulants”. We observe that

- the like-sign and opposite-sign functions have a very similar multiplicity dependence, which is surprising because of their different shapes and assumed origins,
- there exist two regions, one at small  $Q$ , where the multiplicity dependence of both is smaller than  $1/N$ , and one at large  $Q$  ( $\gtrsim 1$  GeV/c), where the functions are negative and follow roughly an  $1/N$  law.

Theoretical work<sup>2,3,12</sup> is challenged by these findings. The similar behaviour of  $\ell s$  and  $os$  functions at small  $Q$ , both decreasing with multiplicity, favours suppression of Bose-Einstein correlations between products of different strings. Resonance decays (Regge terms) should arguably contribute also to  $\ell s$ -functions<sup>8,13</sup>. One could therefore try to explain alternatively the decrease of

$\ell s$  functions with  $N$  by a mixture of Bose-Einstein correlations (assumed to be constant in  $N$ ) with resonance production. This leaves unexplained, however, the similar behaviour of  $os$  and  $\ell s$  functions and the nearly  $N$  independent shape<sup>c</sup> in the small- $Q$  region.

### Acknowledgements

We thank T. Csörgö and his team for their kind hospitality and support. This work was funded in part by the Foundation for Research Development.

### References

1. A. De Angelis, Proc. 27th. Int. Symp. on Multiparticle Dynamics, Frascati, Italy, Sept. 1997.
2. B. Andersson and W. Hofmann, *Phys. Lett.* **B169**,364 (1986).
3. B. Andersson and M. Ringnér, preprint LUTP 97-07, *hep-ph/9704383*; J. Häkkinen and M. Ringnér, preprint LUTP 97-32.
4. L. Lönnblad and T. Sjöstrand, preprint LUTP 97-3, *hep-ph/9711460*.
5. P. Lipa, H.C. Eggers, and B. Buschbeck, *Phys. Rev.* **D53**, R4711 (1996).
6. C. Albajar et al. (UA1), *Z. Phys.* **C44**, 15 (1989); M. Calvetti et al., *IEEE Trans. Nucl. Science NS-30*, 71 (1983).
7. P. Lipa et al., *Phys. Lett.* **B285**, 300 (1992); H.C. Eggers et al., *Phys. Lett.* **B301**, 298 (1993); H.C. Eggers et al., *Phys. Rev.* **D48**, 2040 (1993).
8. We thank A. Białas and K. Fiałkowski for discussions on this topic.
9. C. Albajar et al. (UA1), *Phys. Lett.* **B226**, 410 (1989).
10. T. Åkesson et al. (AFS), *Phys. Lett.* **B187**, 420 (1987).
11. A. Breakstone et al. (SFM), *Z. Phys.* **C33**, 333 (1987).
12. N. Suzuki, this conference.
13. E.L. Berger et al., *Phys. Rev.* **D15**, 206 (1977).

---

<sup>c</sup>The reported increase<sup>9,10,11</sup> of  $R$  with  $N$  is dependent on the choice of the fit function and region. Excluding the region  $Q \geq 1$  GeV/c we observe at small  $Q$  only a minimal or even missing increase of  $R$  (from fits to (13)) with  $N$ .